HHS Public Access

Author manuscript

Cell Tissue Res. Author manuscript; available in PMC 2020 June 01.

Published in final edited form as:

Cell Tissue Res. 2019 June ; 376(3): 325–340. doi:10.1007/s00441-019-03002-0.

Intestinal nerve cell injury occurs prior to insulin resistance in female mice ingesting a high fat diet

Yvonne Nyavor[1], **Rachel Estill**[1], **Hannah Edwards**[1], **Hailey Ogden**[1], **Kaila Heideman**[1], **Kiefer Starks**[1], **Christopher Miller**[1], **George May**[1], **Lance Flesch**[1], **John McMillan**[1], **Martin Gericke**[2], **Larry Forney**[1], and **Onesmo Balemba**[1]

[1]Biological Sciences Department, University of Idaho, 875 Perimeter Drive, LSS 252, Moscow, ID 83844

[2]Institute for Anatomy, University of Leipzig, Liebigstraße 13, 04103 Leipzig, Germany

Abstract

Diabetic patients suffer from gastrointestinal disorders associated with dysmotility, enteric neuropathy and dysbiosis of gut microbiota, however gender differences are not fully known. Previous studies show that high-fat diet (HFD) causes type two diabetes (T2D) in male mice after 4–8 weeks, but only does so in female mice after 16 weeks. This study sought to determine whether sex influences the development of intestinal dysmotility, enteric neuropathy and dysbiosis in mice fed HFD.

We fed 8-week old C57BL6 male and female mice a standard chow diet (SCD) or a 72% Kcal HFD for 8 weeks. We analyzed the associations between sex and intestinal dysmotility, neuropathy and dysbiosis using motility assays, immunohistochemistry and next generation sequencing.

HFD ingestion caused obesity, glucose intolerance and insulin resistance in male but not female mice. However, HFD ingestion slowed intestinal propulsive motility in both male and female mice. This was associated with decreased inhibitory neuromuscular transmission, loss of myenteric inhibitory motor neurons, and axonal swelling and loss of cytoskeletal filaments. HFD induced dysbiosis and changed the abundance of specific bacteria, especially *Allobaculum*, *Bifidobacterium* and *Lactobacillus*, which correlated with dysmotility and neuropathy. Female mice had higher immunoreactivity and numbers of myenteric inhibitory motor neurons, matching larger amplitudes of inhibitory junction potentials.

Correspondence to: Onesmo Balemba (BVM, MVM, PhD), University of Idaho, Department of Biological Sciences, 875 Perimeter Drive, LSS 252, Moscow, ID 83844, obalemba@uidaho.edu.

Author Contributions: Conception and design: YN, LF and OB. Development of methodology: YN, MG and OB. Acquisition of data: YN, RE, KS, CM, HE, KH, HO, JM, GM, MG and OB. Analysis and interpretation of data: YN, MG and OB. Writing, review and/or revision of the manuscript: YN, LF, MG and OB. Study supervision: OB.

Competing Interests On behalf of all authors, the corresponding author states that there is no conflict of interest.

Disclosures: All authors have no competing interests financial or otherwise and have nothing to disclose.

Ethical approval: All applicable international, national, and/or institutional guidelines for the care and use of animals were followed and all procedures performed in studies involving animals were in accordance with the ethical standards of the University of Idaho.

Ethical Statement: All authors declare that this research was done by strictly adhering to the rules of good scientific practice and are responsible for its content. All experiments were performed in a manner that maximized rigor and reproducibility, and without bias.

This study suggests that sex influences the development of HFD-induced metabolic syndrome, but dysmotility, neuropathy and dysbiosis occur independent of sex, and prior to T2D conditions. Gastrointestinal dysmotility, neuropathy and dysbiosis might play a crucial role in the pathophysiology of T2D in humans irrespective of sex.

Keywords

gut microbiota; diabetes mellitus; gastrointestinal motility; enteric nervous system; diabetic enteric neuropathy

INTRODUCTION

Of the 422 million adults living with diabetes globally, 85% are overweight and 90–95% have type 2 Diabetes (T2D)(Centers for Disease Control and Prevention 2017). These individuals are at great risk of life-threatening complications autonomic nerve cell damage-(neuropathy-) related conditions including: cardiovascular disease, and gastrointestinal (GI) motility disorders(Smyth and Heron 2006). In fact, up to 70% of T2D patients suffer from symptoms of GI dysmotility including dysphagia, gastroparesis, constipation, diarrhea and fecal incontinence, and pain as a result of neuropathy of the enteric nervous system (ENS) (Abrahamsson 1995; Yarandi and Srinivasan 2014).

Damage to the myenteric plexus causing axonal swelling and loss of cytoskeletal filaments, disorganization of the neuropil, and loss of myenteric inhibitory motor (VIP/nNOS) neurons due to apoptosis or necrosis (Anitha et al. 2006; Stenkamp-Strahm et al. 2013) is associated with dysmotility. This is because myenteric neurons play a crucial role in regulating gastrointestinal motility mainly by signaling contraction and relaxation of smooth muscle, and coordinating propulsive movements (Kunze and Furness 1999; Furness 2012).

High fat diet (HFD) animal models are commonly used to study T2D, diabetic ENS neuropathy and accompanying dysmotility because T2D is commonly associated with consuming a high fat western diets (Cefalu 2006). In addition, HFD-induces diabetic ENS injuries in both laboratory mice and rats (Voss et al. 2013; Stenkamp-Strahm et al. 2013; Stenkamp-Strahm et al. 2015) that correlate with ENS injuries in diabetic (T2D) humans (Chandrasekharan et al. 2011; Grover et al. 2011; Farrugia 2015). In both animal models and humans, ENS injuries are attributed to oxidative stress induced by hyperglycemia and inflammation(Vincent et al. 2004; Chandrasekharan and Srinivasan 2007). However, new studies link ENS injuries elicited by HFD ingestion and T2D with dysbiosis of bacterial communities in the gut through synergist actions of LPS and the saturated fatty acid, palmitate (Everard et al. 2014; Reichardt et al. 2017; Van Hul et al. 2017). Increasing evidence also suggests that molecules such as saturated fatty acids (palmitate), microbial metabolites, and lipopolysaccharide (LPS) have a fundamental role in the pathophysiology of T2D, obesity, and the accompanying GI neuropathy and dysmotility (Cani et al. 2007; Voss et al. 2013; Aziz et al. 2013; Reichardt et al. 2017). Additionally, it is believed that disruption of GI motility and neuropathy occurs before overt symptoms of obesity and T2D(Nyavor and Balemba 2017; Reichardt et al. 2017). This suggests a need for a better

understanding of the relationship between diet, gut microbiota, GI neuropathy and dysmotility in T2D.

The gut microbiota play a role in the development of the ENS, and establishing a healthy ENS and maintaining normal GI motility (Grenham et al. 2011; Aziz et al. 2013; Collins et al. 2014). Dysbiosis of the gut microbial community has been linked to several motility disorders(Quigley 2011; Kashyap et al. 2013) but the association between gut microbial composition, intestinal dysmotility and nerve cell damage in T2D is not known. The composition of the gut microbiome is shaped by diet, gender and body mass index (Kashyap et al. 2013; Haro et al. 2016). Previous studies suggest that gender (sex) also plays a role in the incidence and disease severity of obesity and T2D, resultant complications including GI motility disorders and deaths attributed to T2D in humans (Kearney et al. 2004; Ford 2005; Sugiyama and Agellon 2012). Additionally, in mouse models of HFD obesity and T2D, female mice fed HFD for eight weeks do not develop hyperglycemia, hyperinsulinemia and low-grade inflammation (Pettersson et al. 2012; Morselli et al. 2014; Bridgewater et al. 2017). In contrast, male mice become obese and exhibit hyperglycemia, hyperinsulinemia and inflammation. Collectively, these observations suggest that dysbiosis of the gut microbial community and gender could influence the incidence of GI neuropathy and dysmotility in both diabetic animal models and humans.

The aims of this study were to: a) determine whether 8 week HFD ingestion in male and female C57BL6 mice disrupts duodenal and colon motility by injuring myenteric inhibitory motor neurons, and reducing inhibitory neuromuscular transmission prior to overt diabetes; b) determine if altered intestinal propulsive motility, neuropathy and gut dysbiosis are correlated; and c) determine whether there gender differences.

MATERIALS AND METHODS

Mice

The University of Idaho Animal Care and Use Committee approved all study procedures. Seven week-old male and female C57Bl/6J mice were purchased from Jackson Laboratories (Bar Harbor, ME), and housed in the Laboratory Research Animal Facility. Mice were split into two groups and fed either a standard chow diet (SCD) composed of 6.2% fat (Teklad Global 2018, Teklad Diets, Madison WI) or a HFD containing 45% fat (70% kcal from lard plus 2% kcal from corn oil, TestDiet, Richmond, IN) *ad libitum* for 8 weeks (Supplementary Table S1). Mice were euthanized by exsanguination under deep isoflurane anesthesia.

Obesity and T2D assessment

Weights of mice were monitored weekly throughout the study. Hyperglycemia was assessed every two weeks using an Abbott AlphaTrak glucometer (Abbott Park, IL). Glucose intolerance was assessed by intra-peritoneal glucose tolerance test at 8 weeks as previously described (Stenkamp-Strahm et al. 2013). Briefly, after fasting mice for 6 hours during the onset of light cycle, blood was drawn from a tail vein and blood glucose (BG) values were obtained using an Abbott AlphaTrak glucometer. Each mouse received an intra-peritoneal injection of glucose solution (1 g/kg–1) and BG values were measured at 30, 60, 90 and 120

minutes after by tail vein blood draw. Homeostatic model (HOMA) values were generated to measure insulin resistance in mice as previously described (Matthews et al. 1985). To measure insulin, on the day of euthanasia, mice were fasted for 4 hours during the light cycle and blood was collected from a submandibular vein. BG values were measured and serum was collected and stored at −80°C. Serum insulin values were measured using a Milliplex kit (Billerica, MA).

Measuring intestinal motility (motility assays)

All motility assays were conducted using the Gastrointestinal Motility Monitoring system (GIMM, Med-Associates Inc., Saint Albans, VT) for filming duodenal contractions triggered by intraluminal superfusion of Krebs, and pellet propulsion in colon as previously described (Balemba et al. 2010; Hoffman et al. 2010). Briefly, approximately 6 cm long duodenum segments and the whole large intestine from cecum to the anus were immediately removed from euthanized animals and placed in ice-chilled Krebs solution. Each sample was pinned on either end in a Sylgard-lined 50 mL organ bath, continuously perfused with oxygenated Krebs solution (mmol L^{-1}: NaCl, 121; KCl, 5.9; CaCl2, 2.5; MgCl2, 1.2; NaHCO3, 25; NaH2PO4, 1.2; and glucose, 8; all from Sigma, St. Louis, MO, USA; aerated with 95% O_2/5% CO_2) at a rate of 10 mL per minute and maintained at temperatures between 35 and 36 °C. Duodenal segments were cannulated and intraluminally superfused with Krebs (kept at room temperature) at a flow rate of 1 mL min^{-1} to trigger propagating contractile rings. Contraction velocities were determined by recording videos of contractions migrating from the oral to aboral end of the segment after a thirty-minute equilibration, and constructing spatiotemporal maps as previously described (Wu et al. 2013). Contraction frequency was determined as the number of contractions per second in spatiotemporal maps.

Colon motility was performed using mouse fecal pellets coated with nail polish. The whole colon was pinned loosely in the tissue bath, and after 20 minutes of equilibration, nail polish coated pellets were inserted in the oral end and videos of the pellet moving through the intestine were recorded. We then used GIMM to determine the pellet propulsion velocity by calculating the time taken by the pellet to travel over a minimum distance of 4 cm in the aboral direction of the colon.

Measurement of inhibitory junction potentials (IJPs)

One cm long segment of oral distal colon was pinned in Krebs solution in a Sylgard-lined petri dish and opened along the mesenteric border. The sample was transferred into a recording chamber, pinned-stretched mucosal surface up and mucosal and submucosal layers were teased off with sharp forceps and mounted in a recording chamber. Roughly, 1.3 cm long × 1.0 cm wide samples of colon muscularis externa were pinned stretched between two parallel stainless steel stimulating electrodes (# 571000; A-M Systems, Sequim, WA) in Sylgard-lined 3.5 mL recording chambers, mucosal surface up. They were pinned between two electrodes for triggering electrical field stimulation. One electrode was placed at near the oral and another electrode was placed at close to the aboral ends. Samples were then mounted on an inverted Nikon Ti-S microscope and visualized using ×20 objective. IJPs were evoked by single electrical field stimulation (train duration, 500 ms; frequency, 10 Hz; pulse duration, 0.8 ms; and voltage, 100 V) using established procedures (Spencer et al.

2001; Bhattarai et al. 2016). IJPs were measured in the circular muscle by using glass microelectrodes (80–120 MΩ tip resistance). Recording was done at 0.5–0.8 cm from the aboral end of each sample.

Preparation of Tissues for immunohistochemistry analysis

After motility assays, tissues were placed in ice-chilled HEPES buffer (mmol L-1: NaCl 134; KCl 6; CaCl2 2; MgCl2 1; HEPES 10; Glucose 10), immediately opened along the mesenteric border, stretched mucosa side-up and pinned flat in Sylgard (Dow Corning, Midland, MI) lined glass dishes. Tissues were fixed in 4% paraformaldehyde with 0.2% picric acid overnight at 4 °C. They were washed three times for 30 minutes each in 1× PBS and stored in 1× PBS with 0.01 M sodium azide (NaN3). 2 cm long oral segments of duodenum and distal colon were dissected under a stereomicroscope using fine forceps to obtain longitudinal muscle-myenteric plexus (LMMP) whole-mount preparations. Preparations were stored at 4 °C in 1× PBS containing 0.01 M NaN3.

Immunohistochemical staining

Immunohistochemistry staining for nitric oxide synthase (nNOS, Abcam, Cambridge, MA) and vasoactive intestinal peptide (VIP, Abcam, Cambridge, MA) to localize myenteric inhibitory motor neurons was performed as previously described (Stenkamp-Strahm et al. 2013). LMMPs were washed 6 × 20 minutes each in 1× phosphate buffered solution with 0.5% Triton X. Tissues were then incubated in 5% Normal Donkey serum overnight, and then in primary antibody solutions for 48 hours. After 6 × 20 minutes washes, tissues were incubated in secondary antibody solution for 3 hours, washed 3 × 20 minutes each and mounted. Total neuron population analysis was completed using an antibody for anti-neuronal nuclear antibody 1 (ANNA1 positive human serum, kind gift from Dr. Vanda A. Lennon, Mayo Clinic). ANNA1 positive serum was pre-adsorbed for 2 hours in beef liver powder and used at 1:20,000 to co-label tissues stained with nNOS and VIP. We used Donkey anti-rabbit 594 and donkey anti-human 488 secondary antibodies (Jackson ImmunoResearch, West Grove, PA), both at 1:300, to stain for nNOS/VIP and ANNA1, respectively.

Tissues were mounted on objective slides using VectaShield Mounting Medium (Vector Labs, Burlingame, CA).

Measuring the packing density and density indices in myenteric ganglia

Myenteric ganglia were visualized with both TRITC and FITC filters and photographed using a wide field camera on a Nikon/Andor Spinning disk microscope with a 40× objective lens (Nikon, Melville, NY). Images were analyzed with Nikon NIS Elements software using the approach we previously described (Stenkamp-Strahm et al. 2013). Briefly, at least 60 fields of view were uniformly randomly selected per tissue and marker. Ganglionic areas were measured and recorded as described previously (Stenkamp-Strahm et al. 2015). Then, nNOS and ANNA1 positive neurons per ganglia were counted and used to generate neuronal densities (number of neurons/ganglionic area; packing density). For both nNOS and VIP stained LMMPs, images were manually thresholded to allow software to detect only stained neurons and nerve fibers (immunoreactive varicosities) within the ganglia, and this area was

measured to compute density index (stained area/ganglionic area). To determine changes in ganglionic size, average ganglionic sizes were calculated using ganglionic areas measured from all images. Images for qualitative demonstration of nNOS, VIP and ANNA1 staining were acquired with a 60× objective lens with the Nikon Spinning disk laser confocal microscope and Nikon NIS elements acquisition software.

Analysis of nerve cell injury by Transmission Electron Microscopy (TEM)

Approximately 0.5 cm long, oral duodenal segments were cut along the mesenteric border, pinned flat and fixed in 2.5% glutaraldehyde with 4% paraformaldehyde (Electron Microscopy Sciences, Hatfield, PA) for 24 hours at 4 °C. Tissues were washed three times in 1× PBS, sectioned, stained and mounted as we previously described (Stenkamp-Strahm et al. 2013). Image acquisition and analysis were done using a Zeiss SIGMA electron microscope (Zeiss, Germany). After washing tissues three times in 1× PBS, they were dehydrated in graded ethanol and stained with OsO4 and uranyl acetate. Tissues were then embedded in Durcupan Fluka resin and polymerization for 48 hours at 56 °C. Tissue blocks were trimmed and cut into ultrathin 55 nm sections on an ultra-microtome. After collection on Formvar-coated single-slot grids, sections were incubated in lead citrate. Imaging was conducted on a Zeiss Sigma electron Microscope (Zeiss, Germany).

Analysis of the gut microbiota by 16S rRNA sequencing and taxonomic assignment of reads

Genomic DNA was extracted from fecal pellets using enzymatic and mechanical lysis as previously described (Yuan et al. 2012). Fecal pellets from individual mice were collected in sterile containers and stored at −80°C. All pellets were then thawed on ice and one pellet (~ 38mg) per mouse transferred into a sterile 2.0 mL glass tube with cell lysis buffer composed of 50 μL lysozyme (10 mg/ml, Sigma-Aldrich, St. Louis, MO, USA), 6 μL mutanolysin (25 KU/ml; Sigma-Aldrich, St. Louis, MO, USA), and 3 μL lysostaphin (4000 U/ml, Sigma-Aldrich, St. Louis, MO, USA) and 41 μL of TE50 buffer (10 mM Tris·HCl and 50 mM EDTA, pH 8.0). After incubating at 37°C for 1 hour, pellets were mechanically disrupted by vortexing at high speed. 600 mg of 0.1-mm-diameter zirconia/silica beads (BioSpec, Bartlesville, OK, USA) were added to the mixture to lyse bacterial cells by using Mini-BeadBeater-96 (BioSpec) at 2100 rpm for 1 minute. Further isolation and purification of the total genomic DNA from crude lysates were processed using QIAamp DNA Mini Kit (Qiagen, Hilden, GER) according to the manufacturer's handbook except that DNA was eluted into two separate tubes using two 100 μL aliquots. A Nanodrop 2000 was used to quantify genomic DNA in each sample according to manufacturer's instructions (Thermo Fisher Scientific, Waltham, MA, USA). Thereafter, DNA was purified on the Qiagen fecal DNA kit (Qiagen, Venlo, Netherlands). Bacterial 16S rRNA genes were amplified by PCR using barcoded primers flanking hypervariable regions V1 to V3 (*Escherichia coli* positions 27F to 534R). The variable V1–V3 regions of 16S rRNA genes in each sample were amplified in two rounds of PCR with dual barcode indexing prior to analysis on an Illumina MiSeq platform (Illumina, San Diego, CA, USA). The first PCR round amplified the target specific regions in 16S rRNA genes (E. coli positions 27F-534R), while the second attached sample specific barcodes and Illumina sequencing adapters. The V1–V3 regions of 16S rRNA genes were amplified in 96-well microtiter plates using the HotStar HiFidelity PCR

kit (Qiagen) and 100 ng of template DNA in a total reaction volume of 50μl with the universal 16S rRNA primers 27F and 534R. The first round of PCR was run in a PTC-100 thermal controller (MJ Research, St. Bruno, Quebec, CAN) using the following cycling parameters: 2 min of denaturation at 95°C, followed by 20 cycles of 1 min at 95°C (denaturing), 1 min at 51 °C (annealing), and 1 min at 72 °C (elongation), with a final extension at 72°C for 10 min. The presence of amplicons was confirmed by agarose gel electrophoresis and staining with Gel Red. The second PCR was run in a total reaction volume of 20μl using the following cycling parameters: 10 min of denaturation at 95°C, followed by 10 cycles of 15 s at 95°C (denaturing), 30 s at 51 °C (annealing), and 1 min at 72 °C (elongation), with a final extension at 72 °C for 3 min. Negative controls without a template were included for each primer pair. The following procedure was performed by the Genomics Resources Core of the Institute for Bioinformatics and Evolutionary Studies (IBEST) at the University of Idaho: Amplicon concentrations were quantified by fluorometry (GeminiXPS, Molecular Devices, Sunnyvale, CA, USA) using PicoGreen, then equimolar amounts of the PCR amplicons were pooled in a single tube. Short DNA fragments and amplification primers were removed from the pool amplicons using AMPure beads (Beckman-Coulter, Indianapolis, IN, USA), and then the purified amplicons were qualified on an Advanced Analytical Fragment Analyzer (Ankeny, IA). This cleaned amplicon pool was then quantified using the KAPA Illumina library quantification kit (KAPA Biosciences, Wilmington, MA, USA) on the Applied Biosystems StepOnePlus real-time PCR system. This concentration was used as a starting point to normalize the pool to 10nM. Amplicons were sequenced using an Illumina MiSeq platform and a 300bp paired-end protocol (Illumina, Inc., San Diego, CA) with custom sequencing primers. dbcAmplicons were used to demultiplex all amplicons from other reads in the run after identifying the dual-barcoded pair, and further by using the locus-specific primers as an additional “barcode.” The final amplicons were sequenced using the Illumina MiSeq platform (Illumina, San Diego, CA, USA) at the University of Idaho.

Sequence reads were cleaned, filtered, and taxonomically assigned using the Ribosomal Database Project (RDP) (http://rdp.cme.msu.edu) Naive Bayesian Classifier to the first RDP level with a bootstrap score of ≥50 for phylum to genus classification. Data were then processed using R scripts to calculate taxon relative abundance based on the total number of sequences within each sample. To simplify community composition analysis, we only included taxa constituting: a) at least 1% of the community in two or more samples or b) 5% of the community in at least one sample. Taxonomically assigned reads that did not meet this threshold were combined into an “Other Bacteria” category, along with reads that could not be taxonomically assigned beyond the level of bacteria. Qualitative assessments of changes in genus-level community richness and diversity were performed by calculating Shannon’s and Simpson’s indices(Payne et al. 2011). Hierarchical clustering and principal components analysis (PCoA) (Ravel et al. 2011) were used to assess similarities and differences in bacterial community composition across HFD male and female mice.

Statistical analysis

Statistical analyses were performed using GraphPad Prism 5 software (GraphPad Software Inc, La Jolla, CA) unless otherwise indicated. A two-tailed unpaired Student’s t-test was

used to compare means of SCD and HFD mice. A repeated measure ANOVA with Bonferroni post-hoc test was used to correct for multiple comparisons. Correlations were performed with a Spearman's correlation matrix on average data for each group of test animals. Statistical significance was determined at $P < 0.05$. Similarities in gut bacterial communities' composition were assessed with Ward's linkage and Hellinger distance and hierarchical clustering using R. Principal Coordinates analysis (PCoA) was used to assign the variability of samples in the dataset to a reduced set of variables termed principal coordinates (PCs). Gut microbial communities in male and female mice fed SCD and HFD were compared by PCoA utilizing computed Euclidean distances. The first two PCs were used to map each sample in a two dimensional space.

Data in bar graphs are expressed as mean ± SEM and analyzed by one-way analysis of variance followed by Tukey's post-tests. In addition, we performed correlation analysis between average relative abundance of bacteria and duodenal contraction velocity, number of nNOS neurons per ganglionic area in duodenum, colonic pellet propulsion velocity and number of nNOS neurons per ganglionic area in the colon. A correlation matrix generated by computing Pearson's coefficient was used to determine r and p values. Data is presented in tables.

Results

HFD ingestion for 8 weeks caused obesity and type 2 diabetes in male but not female mice.

To determine if HFD induced conditions associated with type two diabetes in both male and female mice in a similar manner after 8 weeks, we monitored weight gain, glucose intolerance, insulin sensitivity and levels of leptin, resistin and plasmogen activator inhibitor 1 (PAI1) in both SCD and HFD mice. The mean weight gained by male mice on HFD was statistically higher than that of male mice fed SCD after 8 weeks (Fig. 1a). Female mice fed HFD gained similar amounts of weight as those fed SCD. Immediately after euthanasia, epididymal fat pads were collected, weighed, and computed as a fraction of total mouse body weight. Compared to SCD mice, fat pad weights were found to be higher only in HFD male mice (Fig. 1b). Compared to the SCD group, after 8 weeks on HFD, male mice had impaired glucose tolerance and had higher HOMA values, indicating insulin resistance (Fig. 1c–d). In contrast, female mice on HFD had identical glucose tolerance and HOMA values to that of SCD female mice, suggesting HFD did not cause impaired glucose tolerance and insulin resistance in female mice. Additionally, while leptin concentrations were elevated in the serum of both male and female HFD mice, only HFD male mice had elevated levels of resistin and plasmogen activator inhibitor 1 (PAI1) (Supplementary Fig. 1a–c). Taken together, these findings suggest that HFD caused obesity, impaired glucose tolerance, insulin resistance and inflammation in male, but not female, mice after 8 weeks.

HFD ingestion slowed intestinal propulsion in male and female mice.

To determine if HFD consumption affected intestinal motility in both male and female mice, we measured duodenal and colon motility *ex vivo*. Contraction velocities were significantly reduced in the small intestine of both HFD male and female mice (Fig. 2a). Importantly, the

duodenums of HFD mice of both sexes were unable to relax and contract properly (Supplementary Fig. 2a–f). Colonic pellet propulsion velocities were significantly reduced in both HFD male and female mice (Fig. 2b). These results suggest that HFD ingestion reduces intestinal propulsion in male and female mice. Slowed intestinal propulsion occurred before the development of obesity, impaired glucose tolerance, and insulin resistance in female mice.

HFD ingestion diminished inhibitory neuromuscular transmission in male and female mice.

Previous studies suggest that diabetes and HFD dysmotility is caused by diminished inhibitory neuromuscular transmission as a result of damage to myenteric inhibitory motor, which release the inhibitory neurotransmitters NO and VIP to signal smooth muscle relaxation (Bhattarai et al. 2016). NO and VIP act by triggering smooth muscle membrane hyperpolarizations termed inhibitory junction potentials (IJPs) (Spencer et al. 2001; Bhattarai et al. 2016). To analyze whether HFD disrupted relaxation by reducing IJPs, intracellular microelectrode recordings was used to measure IJPs in circular smooth muscle cells of the distal colon. We observed that the amplitudes and durations of IJPs were significantly reduced in both HFD male and female mice (Fig. 2c–f). Noteworthy, IJPs amplitudes were significantly larger in SCD female mice than SCD male mice (Fig. 2c–e). These results suggest that colonic IJPs were affected similarly by HFD ingestion regardless of gender and the absence of obesity and T2D conditions in female mice. Interestingly, female mice appear to have greater inhibitory neuromuscular transmission to colon circular muscle than male mice.

HFD ingestion damages inhibitory motor neurons in the intestine of male and female mice.

To further analyze the effect of HFD on myenteric inhibitory motor neurons, we determined if HFD damaged and reduced the number of myenteric inhibitory motor neurons in both male and female mice. This was achieved by analyzing the effect of HFD on nNOS, VIP and total number of neurons (ANNA-1 positive neurons) in LMMPs from duodenums and colons. The numbers of nNOS positive neurons, and the area of nNOS immunoreactive neurons and varicosities (nNOS density index), were significantly reduced in the duodenums and colons of both HFD male and female mice (Fig. 3a–h). Additionally, the VIP density index of HFD male and female mice was significantly lower than that of SCD mice in both duodenum and colon (Fig. 4a–f). HFD also reduced ANNA-1 positive cells per ganglionic area in the duodenum and colon of male and female mice (Fig. 5a–b). Of note, female mice had greater nNOS density indices compared to male mice in the duodenum and colon (Fig. 3b, d), greater VIP density index in colon (Fig. 4b) and number of neurons per ganglionic area in colon (Fig. 5b).

To compare HFD effects on myenteric neurons further, we analyzed the ultrastructure of duodenal myenteric ganglia by TEM (Fig. 5g–j). We observed regular morphology of nerve fibers in SCD male and female mice (Fig. 5g, 5i). The myenteric plexus of HFD male and female mice exhibited axonal swelling as well as loss of neurofilaments and microtubules. These ultra-structural alterations in HFD-fed mice were more noticeable in males than

females (Fig. 5h, 5j). Collectively, these findings show that damage to the ENS precedes development of obesity and T2D conditions in female mice.

HFD alters the composition of gut microbial community of both male and female mice in a similar manner.

The dysbiosis of the gut microbiota is associated with diabetes and intestinal(Kashyap et al. 2013; Ussar et al. 2015) dysmotility. We studied the differences in the composition of the fecal microbiota of both male and female mice by classifying bacteria based on 16S rRNA sequences. Clustering analysis revealed that the microbial communities of mice grouped together by diet (SCD vs. HFD clusters), but not by gender (Fig. 6a). PCoA using Euclidean distances confirmed that diet influenced community composition. The first 2 PCs explained approximately 80% and 8% respectively of the variation observed between samples (Supplementary Fig. 3a). These two PCs (clusters) were significantly different from each other (Chi square, $P<0.00001$). In addition, observed community diversity was reduced by HFD ingestion in both male and female mice (Supplementary Fig. 3b–c). Samples in the HFD cluster were defined by a higher observed relative abundance of *Firmicutes*, and lower relative abundances of *Bacteroidetes* and *Actinobacteria*, compared to samples in the SCD cluster (Fig. 6b). At the genus level, HFD ingestion caused a tremendous increase in the relative abundance of *Allobaculum*, and a reduction of the abundance of *Lactobacillus, Bifidobacterium, and Clostridium sensu stricto* (Fig. 6b). Our results suggest that HFD caused a similar pattern of dysbiosis in male and female mice even though female mice did not have obesity, hyperglycemia, glucose intolerance and insulin resistance.

HFD-induced gut microbiota changes correlate with intestinal motility and neuropathy.

To determine the interrelationship between intestinal dysmotility, neuropathy, and gut microbiota changes, we performed correlation and regression analyses. We found that several bacteria, including *Allobaculum*, which were increased by HFD ingestion, were negatively correlated with intestinal motility and nerve cell health (Table 1). Conversely, bacteria with lowered relative abundances in HFD mice, such as *Bifidobacterium*, positively correlated with intestinal motility and nerve cell health (Table 1). All bacteria (except those with relative abundances lower than 1%) that showed significant correlations with intestinal motility and health may be found in Supplementary Tables S2–5. Dysmotility was positively correlated with injury to nNOS neurons both in the duodenum and colon (Supplementary Table S6). Collectively, these results suggest that there are specific interrelationships between intestinal bacteria, motility and myenteric nerve cell health.

DISCUSSION

The purpose of this study was to determine whether slower intestinal propulsive motility, ENS neuropathy, and dysbiosis of the gut microbiota occurred prior to overt diabetes conditions using a HFD mouse model. Consumption of a HFD for 8 weeks caused obesity, hyperglycemia and insulin resistance, and increased leptin, resistin and PAI-1 in male but not female mice. Regardless of these differences in metabolic conditions, both male and female HFD mice exhibited slower intestinal propulsive motility, reduced number of myenteric inhibitory motor neurons in both duodenum and distal colon, and reduced IJPs in

colon. HFD ingestion resulted in dysbiosis of the gut microbiota with an overall loss of observed diversity, an increase in the relative abundance of *Firmicutes* and a reduction in *Bacteroidetes* and *Actinobacteria*. HFD also led to a dramatic increase in the abundance of *Allobaculum* accompanied by a striking reduction of *Lactobacillus*, *Bifidobacterium*, and *Clostridium sensu stricto*. Changes in intestinal motility and neuropathy correlated both positively and negatively with shifts in the abundances of specific members of microbiota irrespective of gender. Taken together, our results suggest that slower intestinal propulsive motility, ENS neuropathy, and dysbiosis of the gut microbiota occur prior to glucose intolerance and insulin resistance. Additionally, we found that gender influences the development of HFD-induced metabolic syndrome but not gastrointestinal dysmotility, neuropathy and dysbiosis, which develops prior to overt T2D.

HFD caused obesity, glucose intolerance, and insulin resistance more rapidly in male than female mice. Obesity, glucose intolerance, and insulin resistance, developed in male mice fed a HFD for 8 weeks but not in female mice. Additionally, unlike female mice, male mice had higher circulating concentrations of resistin and PAI-1. These findings are consistent with previous studies showing that 32%−72% Kcal HFD caused increased weight gain and adiposity, as well as hyperglycemia and insulin resistance as early as 4 weeks in male mice (Stenkamp-Strahm et al. 2013; Reichardt et al. 2017) while female mice were protected from HFD-induced metabolic syndrome (Pettersson et al. 2012; Morselli et al. 2014; Bridgewater et al. 2017). Reasons for these gender differences are not understood, but it is thought that estrogen protects female animals and women against development of the metabolic syndrome and T2D (Ozbey et al. 2002; Morselli et al. 2014). It is also possible that progesterone protects females against obesity, insulin resistance, and T2D by attenuating HFD-induced low-grade inflammation (Lei et al. 2014). Our results are consistent with both of these ideas.

One of our main findings is that despite the lack of obesity and diabetic conditions, HFD females had decreased intestinal motility. The observations in female mice support the view that dysmotility precedes the development of obesity, glucose intolerance and insulin resistance (Nyavor and Balemba 2017; Reichardt et al. 2017). It is likely that dysmotility occurs in humans of both genders prior to overt obesity and T2D because dysmotility in this mouse model of T2D closely matches observations in diabetic humans (Yarandi and Srinivasan 2014). Normal rates and patterns of GI motility are crucial for maintaining gut microbiota homeostasis and body metabolism, because a decreased motility correlates with dysbiosis, and increased nutrient absorption, which exacerbates obesity and T2D conditions (Kashyap et al. 2013; Fu et al. 2014). Disruptions in the rate and pattern of GI motility could therefore play a vital role in the pathogenesis of obesity and T2D conditions.

In both sexes, HFD-induced slower propulsive motility was associated with neuropathy characterized by loss of nNOS neurons, reduced nNOS and VIP varicosities, reduced total number of neurons, axonal swelling and loss of cytoskeletal filaments in the myenteric plexus. Recorded nerve cell injuries and diminished inhibitory neuromuscular transmission match previous findings in HFD male mice (Stenkamp-Strahm et al. 2013; Bhattarai et al. 2016; Reichardt et al. 2017) and diabetic humans (Pasricha et al. 2008; Yarandi and Srinivasan 2014). Moreover, inhibitory neuromuscular transmission (durations and

amplitudes of IJPs) was diminished in both sexes fed HFD. In mouse colon, nitric oxide prolongs the waveform of IJPs, while purines determine IJP amplitudes. Our results suggest decreased availability of nitric oxide caused by injury and loss of nNOS neurons (Bhattarai et al. 2016). Additionally, our results suggest the likelihood of decreased availability of purines due to oxidative stress- and inflammation- induced nerve cell damage (Bertrand et al. 2011; Roberts et al. 2013; Sandireddy et al. 2014). Our results match with previous studies suggesting that injury to interstitial cells of Cajal and enteric neuropathy can occur in the absence of hyperglycemia (Horváth et al. 2005; Rivera et al. 2014; Reichardt et al. 2017). Although inflammation was not evaluated in this study, low serum concentrations of resistin and PAI-1 (thought to mediate inflammation) in female mice support the view that HFD female mice have a delayed development of low-grade systemic inflammation (Pettersson et al. 2012; Lei et al. 2014). However, this claim and the role of inflammation in enteric neuropathy in females need to be studied further. The observation of myenteric nerve cell damage in female mice support the view that dyslipidemia due to saturated fatty acids (primarily palmitate) and LPS (endotoxin from Gram-negative bacteria) trigger damage to enteric neurons and dysmotility (Voss et al. 2013; Reichardt et al. 2017). Overall, our findings suggest the need for a better understanding of whether neuroinflammation, LPS and saturated fatty acids elicit nerve cell injury and dysmotility in the gut before humans develop obesity and T2D.

Significant gender differences may exist in ENS neurochemical composition and function. The results of this study not only demonstrate the features of T2D enteric neuropathy in female mice, but also show a higher number and immunoreactivity of myenteric inhibitory motor neurons, that match with larger IJP amplitudes in female mice than in male mice. The differences appear to be greater in colon compared to duodenum. These differences support previous findings demonstrating sex differences in motility in humans and in jejunum of mice (Degen and Phillips 1996; Meleine and Matricon 2014; France et al. 2016). They support the need for a better understanding of gender differences in ENS neurochemical coding and function.

During the past decade, studies have revealed that diabetes is characterized by specific intestinal microbiota (Turnbaugh et al. 2006; Boulangé et al. 2016). Consistent with findings from previous studies, 16S rRNA sequencing and analysis of the bacterial community in our HFD-mouse model of T2D revealed clustering by diet and not by sex (Turnbaugh et al. 2006; Boulangé et al. 2016). The relative abundance of *Allobaculum*, a gram positive (in the phylum *Firmicutes*), non-spore forming rod shaped bacterium first isolated from the canine gut (Greetham et al. 2004), was dramatically increased by HFD ingestion in both male and female mice. *Allobaculum* produces SCFAs including butyrate and lactate (Tachon et al. 2013), suggesting it has beneficial effects on the host. Additionally, previous studies have linked the increased abundance of this organism to decreased adiposity, weight loss, and an improvement in diabetic symptoms (Van Hul et al. 2017; Li et al. 2017). However, our study found increased *Allobaculum* abundance in HFD mice, and a negative correlation between its abundance and intestinal motility and nerve cell health. This result conflicts with previous studies, but emphasizes the need to study this bacterium more extensively and examine its specific contribution to the pathophysiology of dysmotility and enteric neuropathy in obesity and T2D.

Our study shows significant correlations between gut microbiota dysbiosis, enteric neuropathy and dysmotility. Previous evidence suggests that members of the microbiota modulate GI motility, and enteric neuronal development, function and health (Quigley 2011; Kashyap et al. 2013; Collins et al. 2014). However, the link between specific microorganisms, diabetic dysmotility and enteric neuropathy is still in its infancy. Here, we show that several bacteria have positive and negative associations with GI motility and nerve cell health, both across the whole intestine and specific intestinal organs. While this study did not delve into cause and effect relationships, our results pave the way for future studies to address the missing link in the interaction between diet, specific members of the gut microbiota, specific cells in the gut, and associated diabetic GI dysfunctions.

In conclusion, our results reveal that while female mice do not display HFD effects on glucose metabolism and insulin sensitivity after 8 weeks, they still develop slower intestinal motility, neuropathy and dysbiosis of gut microbiota similar to HFD male mice. Further, we show that gut dysbiosis is associated with intestinal dysmotility and neuropathy. These findings suggest that GI dysmotility and neuropathy develop before T2D conditions (mainly hyperglycemia, glucose intolerance and insulin resistance), and therefore play a role in the pathophysiology of T2D. Future investigations should focus on studying the causes of intestinal neuropathy and dysmotility and their cellular mechanisms, and the interactions between specific microbes, intestinal motility and nerve cells. Such studies are critical to improving our understanding of the gut-microbiota-ENS interrelationships in health and disease.

Supplementary Material

Refer to Web version on PubMed Central for supplementary material.

ACKNOWLEDGEMENTS

We would like to thank Catherine Brands and the UI Laboratory Animal Research Facility staff for assistance during animal handling, Forrest Potter and Ann Norton (IBEST Optical Imaging Core) for assistance with imaging and analysis. We thank Dan New, Dr. Matt Settles, Dr. Celeste Brown, Dr. Ben Ridenhour and the IBEST Genomics Resources Core for help with microbial community analysis. We also thank Dr. Vanda A. Lennon of the Mayo Clinic for the gift of ANNA1 positive human serum.

Funding Information

Grant support: Research reported in this publication was supported by the University of Idaho—Dyess Faculty Fellowship and Institutional Development Awards (IDeA) from the National Institute of General Medical Sciences of the National Institutes of Health under grant numbers P30GM103324 and P20 GM103408.

REFERENCES

Abrahamsson H (1995) Gastrointestinal motility disorders in patients with diabetes mellitus. J Intern Med 237:403–9. doi: 10.1111/j.1365-2796.1995.tb01194.x [PubMed: 7714464]

Anitha M, Gondha C, Sutliff R, Parsadanian A, Mwangi S, Sitaraman SV, Srinivasan S (2006) GDNF rescues hyperglycemia-induced diabetic enteric neuropathy through activation of the PI3K/Akt pathway. J Clin Invest 116:344–56. doi: 10.1172/JCI26295 [PubMed: 16453021]

Aziz Q, Doré J, Emmanuel A, Guarner F, Quigley EMM (2013) Gut microbiota and gastrointestinal health: current concepts and future directions. Neurogastroenterol Motil 25:4–15. doi: 10.1111/nmo.12046 [PubMed: 23279728]

Balemba OB, Bhattarai Y, Stenkamp-Strahm C, Lesakit MSB, Mawe GM (2010) The traditional antidiarrheal remedy, Garcinia buchananii stem bark extract, inhibits propulsive motility and fast synaptic potentials in the guinea pig distal colon. Neurogastroenterol Motil 22:1332–9. doi: 10.1111/j.1365-2982.2010.01583.x [PubMed: 20718943]

Bertrand RL, Senadheera S, Markus I, Liu L, Howitt L, Chen H, Murphy TV, Sandow SL, Bertrand PP (2011) A Western diet increases serotonin availability in rat small intestine. Endocrinology 152:36–47. doi: 10.1210/en.2010-0377 [PubMed: 21068163]

Bhattarai Y, Fried D, Gulbransen B, Kadrofske M, Fernandes R, Xu H, Galligan J (2016) High-fat diet-induced obesity alters nitric oxide-mediated neuromuscular transmission and smooth muscle excitability in the mouse distal colon. Am J Physiol - Gastrointest Liver Physiol 311:G210–G220. doi: 10.1152/ajpgi.00085.2016 [PubMed: 27288421]

Boulangé CL, Neves AL, Chilloux J, Nicholson JK, Dumas M-E (2016) Impact of the gut microbiota on inflammation, obesity, and metabolic disease. Genome Med 8:42. doi: 10.1186/s13073-016-0303-2 [PubMed: 27098727]

Bridgewater LC, Zhang C, Wu Y, Hu W, Zhang Q, Wang J, Li S, Zhao L (2017) Gender-based differences in host behavior and gut microbiota composition in response to high fat diet and stress in a mouse model. Sci Rep 7:10776. doi: 10.1038/s41598-017-11069-4 [PubMed: 28883460]

Cani PD, Amar J, Iglesias MA, Poggi M, Knauf C, Bastelica D, Neyrinck AM, Fava F, Tuohy KM, Chabo C, Waget A, Delmee E, Cousin B, Sulpice T, Chamontin B, Ferrieres J, Tanti J-FJ-F, Gibson GR, Casteilla L, Delzenne NM, Alessi MC, Burcelin R, Delmée E, Cousin B, Sulpice T, Chamontin B, Ferrières J, Tanti J-FJ-F, Gibson GR, Casteilla L, Delzenne NM, Alessi MC, Burcelin R (2007) Metabolic endotoxemia initiates obesity and insulin resistance. Diabetes 56:1761–72. doi: 10.2337/db06-1491 [PubMed: 17456850]

Cefalu WT (2006) Animal models of type 2 diabetes: Clinical presentation and pathophysiological relevance to the human condition. ILAR J 47:186–198. doi: 10.1093/ilar.47.3.186 [PubMed: 16804194]

Centers for Disease Control and Prevention (2017) National Diabetes Statistics Report, 2017 Estimates of Diabetes and Its Burden in the Epidemiologic estimation methods. US Dep Heal Hum Serv 2009–2012. doi: 10.1177/1527154408322560

Chandrasekharan B, Anitha M, Blatt R, Shahnavaz N, Kooby D, Staley C, Mwangi S, Jones DP, Sitaraman SV, Srinivasan S (2011) Colonic motor dysfunction in human diabetes is associated with enteric neuronal loss and increased oxidative stress. Neurogastroenterol Motil 23:131–e26. doi: 10.1111/j.1365-2982.2010.01611.x [PubMed: 20939847]

Chandrasekharan B, Srinivasan S (2007) Diabetes and the enteric nervous system. Neurogastroenterol Motil 19:951–60. doi: 10.1111/j.1365-2982.2007.01023.x [PubMed: 17971027]

Collins J, Borojevic R, Verdu EF, Huizinga JD, Ratcliffe EM (2014) Intestinal microbiota influence the early postnatal development of the enteric nervous system. Neurogastroenterol Motil 26:98–107. doi: 10.1111/nmo.12236 [PubMed: 24329946]

Degen LP, Phillips SF (1996) Variability of gastrointestinal transit in healthy women and men. Gut 39:299–305. doi: 10.1136/gut.39.2.299 [PubMed: 8977347]

Everard A, Lazarevic V, Gaïa N, Johansson M, Ståhlman M, Backhed F, Delzenne NM, Schrenzel J, François P, Cani PD (2014) Microbiome of prebiotic-treated mice reveals novel targets involved in host response during obesity. ISME J. doi: 10.1038/ismej.2014.45

Farrugia G (2015) Histologic changes in diabetic gastroparesis. Gastroenterol Clin North Am 44:31–8. doi: 10.1016/j.gtc.2014.11.004 [PubMed: 25667021]

Ford ES (2005) Prevalence of the metabolic syndrome defined by the International Diabetes Federation among adults in the U.S. Diabetes Care 28:2745–9 [PubMed: 16249550]

France M, Skorich E, Kadrofske M, Swain GM, Galligan JJ (2016) Sex-related differences in small intestinal transit and serotonin dynamics in high-fat-diet-induced obesity in mice. Exp Physiol 101:81–99. doi: 10.1113/EP085427 [PubMed: 26381722]

Fu X-Y, Li Z, Zhang N, Yu H-T, Wang S-R, Liu J-R (2014) Effects of gastrointestinal motility on obesity. Nutr Metab (Lond) 11:3. doi: 10.1186/1743-7075-11-3 [PubMed: 24398016]

Furness JB (2012) The enteric nervous system and neurogastroenterology. Nat Rev Gastroenterol Hepatol 9:286–94. doi: 10.1038/nrgastro.2012.32 [PubMed: 22392290]

Greetham HL, Gibson GR, Giffard C, Hippe H, Merkhoffer B, Steiner U, Falsen E, Collins MD (2004) Allobaculum stercoricanis gen. nov., sp. nov., isolated from canine feces. Anaerobe 10:301–7. doi: 10.1016/j.anaerobe.2004.06.004 [PubMed: 16701531]

Grenham S, Clarke G, Cryan JF, Dinan TG (2011) Brain-gut-microbe communication in health and disease. Front Physiol 2:94. doi: 10.3389/fphys.2011.00094 [PubMed: 22162969]

Grover M, Farrugia G, Lurken MS, Bernard CE, Faussone-Pellegrini MS, Smyrk TC, Parkman HP, Abell TL, Snape WJ, Hasler WL, Ünalp-Arida A, Nguyen L, Koch KL, Calles J, Lee L, Tonascia J, Hamilton FA, Pasricha PJ, NIDDK Gastroparesis Clinical Research Consortium (2011) Cellular changes in diabetic and idiopathic gastroparesis. Gastroenterology 140:1575–85.e8. doi: 10.1053/j.gastro.2011.01.046 [PubMed: 21300066]

Haro C, Rangel-Zúñiga OA, Alcalá-Díaz JF, Gómez-Delgado F, Pérez-Martínez P, Delgado-Lista J, Quintana-Navarro GM, Landa BB, Navas-Cortés JA, Tena-Sempere M, Clemente JC, López-Miranda J, Pérez-Jiménez F, Camargo A (2016) Intestinal Microbiota Is Influenced by Gender and Body Mass Index. PLoS One 11:e0154090. doi: 10.1371/journal.pone.0154090 [PubMed: 27228093]

Hoffman JM, Brooks EM, Mawe GM (2010) Gastrointestinal Motility Monitor (GIMM). J Vis Exp. doi: 10.3791/2435

Horváth VJ, Vittal H, Ordög T (2005) Reduced insulin and IGF-I signaling, not hyperglycemia, underlies the diabetes-associated depletion of interstitial cells of Cajal in the murine stomach. Diabetes 54:1528–33. doi: 10.2337/diabetes.54.5.1528 [PubMed: 15855342]

Kashyap PC, Marcobal A, Ursell LK, Larauche M, Duboc H, Earle KA, Sonnenburg ED, Ferreyra JA, Higginbottom SK, Million M, Tache Y, Pasricha PJ, Knight R, Farrugia G, Sonnenburg JL (2013) Complex interactions among diet, gastrointestinal transit, and gut microbiota in humanized mice. Gastroenterology 144:967–77. doi: 10.1053/j.gastro.2013.01.047 [PubMed: 23380084]

Kearney PM, Whelton M, Reynolds K, Whelton PK, He J (2004) Worldwide prevalence of hypertension: A systematic review. J Hypertens 22:11–19. doi: 10.1097/01.hjh.0000098149.70956.79 [PubMed: 15106785]

Kunze WA, Furness JB (1999) The enteric nervous system and regulation of intestinal motility. Annu Rev Physiol 61:117–42. doi: 10.1146/annurev.physiol.61.1.117 [PubMed: 10099684]

Lei B, Mace B, Dawson HN, Warner DS, Laskowitz DT, James ML (2014) Anti-Inflammatory Effects of Progesterone in Lipopolysaccharide-Stimulated BV-2 Microglia. PLoS One 9:e103969. doi: 10.1371/journal.pone.0103969 [PubMed: 25080336]

Li H, Qi T, Huang Z sen, Ying Y, Zhang Y, Wang B, Ye L, Zhang B, Chen D ling, Chen J (2017) Relationship between gut microbiota and type 2 diabetic erectile dysfunction in Sprague-Dawley rats. J Huazhong Univ Sci Technol - Med Sci 37:523–530. doi: 10.1007/s11596-017-1767-z [PubMed: 28786059]

Matthews DR, Hosker JP, Rudenski AS, Naylor BA, Treacher DF, Turner RC (1985) Homeostasis model assessment: insulin resistance and β-cell function from fasting plasma glucose and insulin concentrations in man. Diabetologia 28:412–419. doi: 10.1007/BF00280883 [PubMed: 3899825]

Meleine M, Matricon J (2014) Gender-related differences in irritable bowel syndrome: potential mechanisms of sex hormones. World J Gastroenterol 20:6725–43. doi: 10.3748/wjg.v20.i22.6725 [PubMed: 24944465]

Morselli E, Fuente-Martin E, Finan B, Kim M, Frank A, Garcia-Caceres C, Navas CR, Gordillo R, Neinast M, Kalainayakan SP, Li DL, Gao Y, Yi C-X, Hahner L, Palmer BF, Tschöp MH, Clegg DJ (2014) Hypothalamic PGC-1α Protects Against High-Fat Diet Exposure by Regulating ERα. Cell Rep 9:633–645. doi: 10.1016/j.celrep.2014.09.025 [PubMed: 25373903]

Nyavor YEA, Balemba OB (2017) Diet-induced dysmotility and neuropathy in the gut precedes endotoxaemia and metabolic syndrome: the chicken and the egg revisited. J Physiol 595:1441–1442. doi: 10.1113/JP273888 [PubMed: 28078679]

Ozbey N, Sencer E, Molvalilar S, Orhan Y (2002) Body fat distribution and cardiovascular disease risk factors in pre- and postmenopausal obese women with similar BMI. Endocr J 49:503–9 [PubMed: 12402983]

Pasricha PJ, Pehlivanov ND, Gomez G, Vittal H, Lurken MS, Farrugia G (2008) Changes in the gastric enteric nervous system and muscle: A case report on two patients with diabetic gastroparesis. BMC Gastroenterol 8:21. doi: 10.1186/1471-230X-8-21 [PubMed: 18513423]

Payne AN, Chassard C, Zimmermann M, Müller P, Stinca S, Lacroix C (2011) The metabolic activity of gut microbiota in obese children is increased compared with normal-weight children and exhibits more exhaustive substrate utilization. Nutr Diabetes 1:e12. doi: 10.1038/nutd.2011.8 [PubMed: 23154580]

Pettersson US, Waldén TB, Carlsson PO, Jansson L, Phillipson M (2012) Female Mice are Protected against High-Fat Diet Induced Metabolic Syndrome and Increase the Regulatory T Cell Population in Adipose Tissue. PLoS One 7:e46057. doi: 10.1371/journal.pone.0046057 [PubMed: 23049932]

Quigley EMM (2011) Microflora modulation of motility. J Neurogastroenterol Motil 17:140–7. doi: 10.5056/jnm.2011.17.2.140 [PubMed: 21602990]

Ravel J, Gajer P, Abdo Z, Schneider GM, Koenig SSK, McCulle SL, Karlebach S, Gorle R, Russell J, Tacket CO, Brotman RM, Davis CC, Ault K, Peralta L, Forney LJ (2011) Vaginal microbiome of reproductive-age women. Proc Natl Acad Sci U S A 108 Suppl:4680–7. doi: 10.1073/pnas.1002611107 [PubMed: 20534435]

Reichardt F, Chassaing B, Nezami BG, Li G, Tabatabavakili S, Mwangi S, Uppal K, Liang B, Vijay-Kumar M, Jones D, Gewirtz AT, Srinivasan S (2017) Western diet induces colonic nitrergic myenteric neuropathy and dysmotility in mice via saturated fatty acid- and lipopolysaccharide-induced TLR4 signalling. J Physiol 595:1831–1846. doi: 10.1113/JP273269 [PubMed: 28000223]

Rivera LR, Leung C, Pustovit RV, Hunne BL, Andrikopoulos S, Herath C, Testro A, Angus PW, Furness JB (2014) Damage to enteric neurons occurs in mice that develop fatty liver disease but not diabetes in response to a high-fat diet. Neurogastroenterol Motil 26:1188–99. doi: 10.1111/nmo.12385 [PubMed: 24952996]

Roberts JA, Durnin L, Sharkey KA, Mutafova-Yambolieva VN, Mawe GM (2013) Oxidative stress disrupts purinergic neuromuscular transmission in the inflamed colon. J Physiol 591:3725–3737. doi: 10.1113/jphysiol.2013.254136 [PubMed: 23732648]

Sandireddy R, Yerra VG, Areti A, Komirishetty P, Kumar A (2014) Neuroinflammation and oxidative stress in diabetic neuropathy: futuristic strategies based on these targets. Int J Endocrinol 2014:674987. doi: 10.1155/2014/674987 [PubMed: 24883061]

Smyth S, Heron A (2006) Diabetes and obesity: the twin epidemics. Nat Med 12:75–80. doi: 10.1038/nm0106-75 [PubMed: 16397575]

Spencer NJ, Hennig GW, Smith TK (2001) Spatial and temporal coordination of junction potentials in circular muscle of guinea-pig distal colon. J Physiol 535:565–78 [PubMed: 11533145]

Stenkamp-Strahm CM, Kappmeyer AJ, Schmalz JT, Gericke M, Balemba O (2013) High-fat diet ingestion correlates with neuropathy in the duodenum myenteric plexus of obese mice with symptoms of type 2 diabetes. Cell Tissue Res 354:381–94. doi: 10.1007/s00441-013-1681-z [PubMed: 23881404]

Stenkamp-Strahm CM, Nyavor YEA, Kappmeyer AJ, Horton S, Gericke M, Balemba OB (2015) Prolonged high fat diet ingestion, obesity, and type 2 diabetes symptoms correlate with phenotypic plasticity in myenteric neurons and nerve damage in the mouse duodenum. Cell Tissue Res 361:411–26. doi: 10.1007/s00441-015-2132-9 [PubMed: 25722087]

Sugiyama MG, Agellon LB (2012) Sex differences in lipid metabolism and metabolic disease risk. Biochem Cell Biol 90:124–141. doi: 10.1139/o11-067 [PubMed: 22221155]

Tachon S, Zhou J, Keenan M, Martin R, Marco ML (2013) The intestinal microbiota in aged mice is modulated by dietary resistant starch and correlated with improvements in host responses. FEMS Microbiol Ecol 83:299–309. doi: 10.1111/j.1574-6941.2012.01475.x [PubMed: 22909308]

Turnbaugh PJ, Ley RE, Mahowald MA, Magrini V, Mardis ER, Gordon JI (2006) An obesity-associated gut microbiome with increased capacity for energy harvest. Nature 444:1027–31. doi: 10.1038/nature05414 [PubMed: 17183312]

Ussar S, Griffin NW, Bezy O, Fujisaka S, Vienberg S, Softic S, Deng L, Bry L, Gordon JI, Kahn CR (2015) Interactions between Gut Microbiota, Host Genetics and Diet Modulate the Predisposition to Obesity and Metabolic Syndrome. Cell Metab 22:516–530. doi: 10.1016/j.cmet.2015.07.007 [PubMed: 26299453]

Van Hul M, Geurts L, Plovier H, Druart C, Everard A, Ståhlman M, Rhimi M, Chira K, Teissedre P-L, Delzenne NM, Maguin E, Guilbot A, Brochot A, Gerard P, Bäckhed F, Cani PD (2017) Reduced obesity, diabetes and steatosis upon cinnamon and grape pomace are associated with changes in gut microbiota and markers of gut barrier. Am J Physiol - Endocrinol Metab 314:10.1152/ajpendo.00107.2017

Vincent AM, Russell JW, Low P, Feldman EL (2004) Oxidative stress in the pathogenesis of diabetic neuropathy. Endocr Rev 25:612–28. doi: 10.1210/er.2003-0019 [PubMed: 15294884]

Voss U, Sand E, Olde B, Ekblad E, Donath M (2013) Enteric neuropathy can be induced by high fat diet in vivo and palmitic acid exposure in vitro. PLoS One 8:e81413. doi: 10.1371/journal.pone.0081413 [PubMed: 24312551]

Wu RY, Pasyk M, Wang B, Forsythe P, Bienenstock J, Mao Y-K, Sharma P, Stanisz AM, Kunze WA (2013) Spatiotemporal maps reveal regional differences in the effects on gut motility for Lactobacillus reuteri and rhamnosus strains. Neurogastroenterol Motil. doi: 10.1111/nmo.12072

Yarandi SS, Srinivasan S (2014) Diabetic gastrointestinal motility disorders and the role of enteric nervous system: current status and future directions. Neurogastroenterol Motil 26:611–24. doi: 10.1111/nmo.12330 [PubMed: 24661628]

Yuan S, Cohen DB, Ravel J, Abdo Z, Forney LJ (2012) Evaluation of methods for the extraction and purification of DNA from the human microbiome. PLoS One 7:e33865. doi: 10.1371/journal.pone.0033865 [PubMed: 22457796]

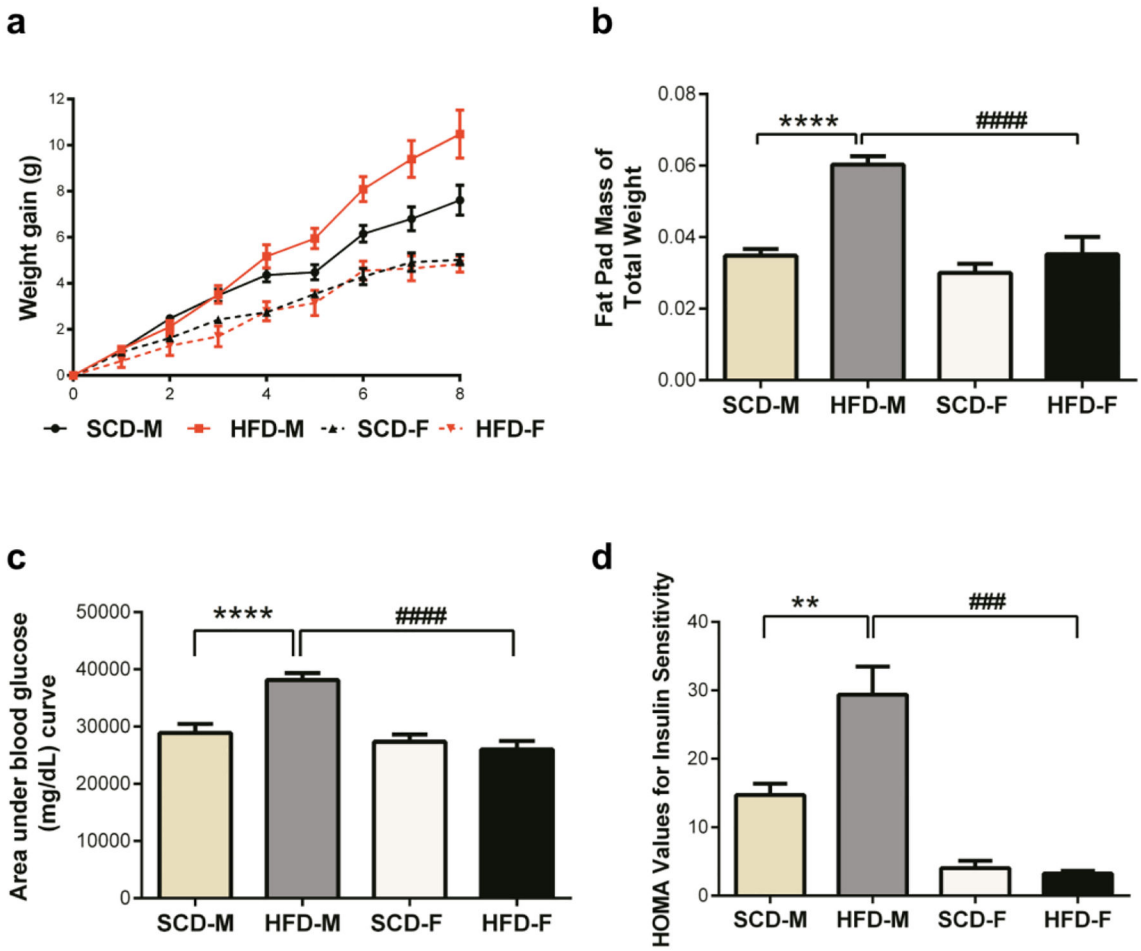

Fig. 1.

HFD has a greater metabolic effect on male mice than on female mice. Male mice fed HFD (HFD-M) gained statistically higher amounts of weight by week 5 (a) than male SCD mice and this persisted till week 8, while female mice (HFD-F) did not gain weight even after 8 weeks (a). Unlike in female mice, intraperitoneal fat pads made up a significantly higher percentage of the body weights of male mice fed HFD (b). Male HFD mice were glucose intolerant at 8 weeks, evidenced by higher area under blood glucose curve (c), while female HFD mice were not. HFD ingestion resulted in insulin resistance in male mice, but not female mice (d). Data are expressed as mean ± SEM and were analyzed by one-way analysis of variance followed by Tukey's post-tests. Here and here after, number of animals for experiments were n=5–10 per group. Symbols denoting statistical significance are: ns = P > 0.05; * P or +P or # P show P≤ 0.05; ** P or ++ P, or ## P show P≤ 0.01; *** P or +++ P or ### P show P ≤ 0.001, while **** P, ++++ and #### P show P value ≤ 0.0001.

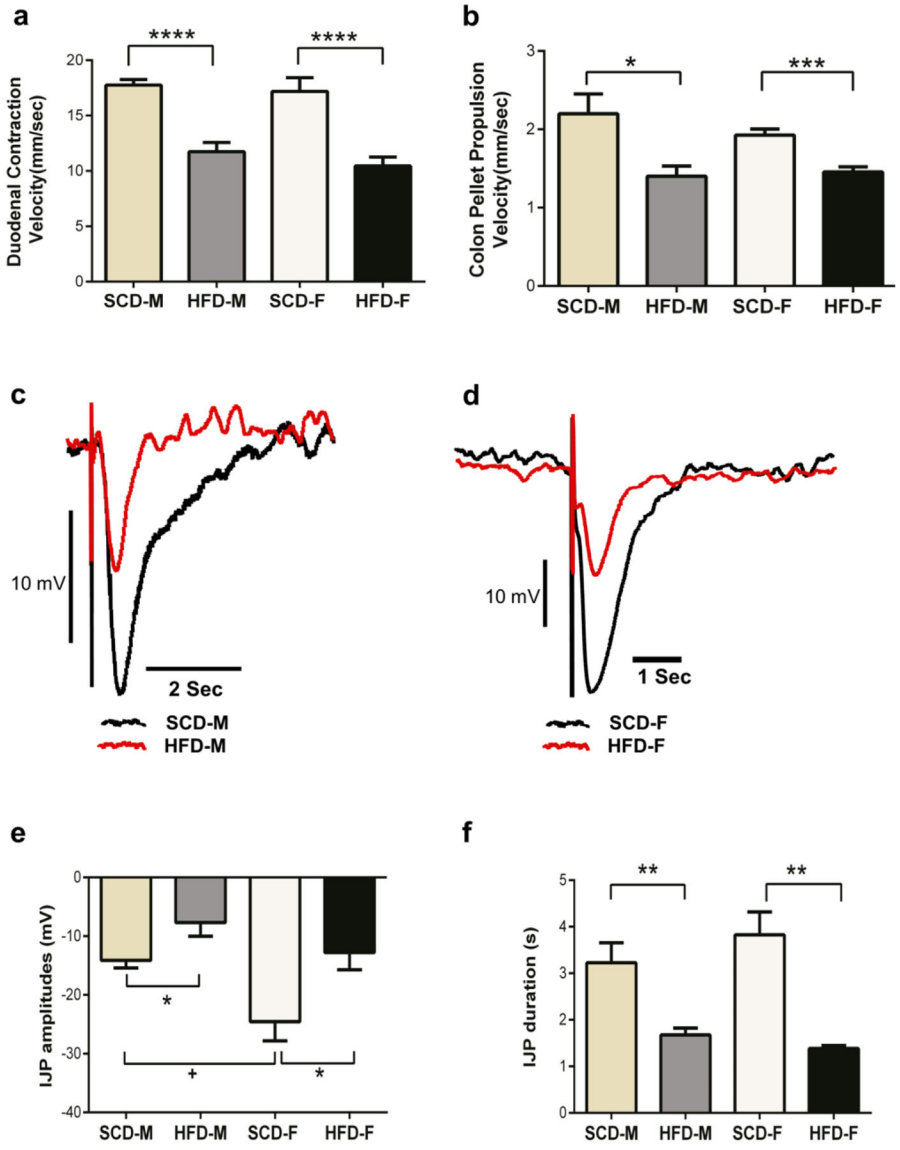

Fig. 2.

HFD results in intestinal dysmotility and disrupts inhibitory intestinal neuromuscular transmission in both male and female mice. Duodenal contraction velocities (a) and colon pellet propulsion velocities (b) were significantly reduced by HFD ingestion in both male and female mice. HFD ingestion resulted in reduced IJP amplitudes and durations in circular smooth muscle cells in colons of both male and female mice (c-f). SCD female mice had larger IJP amplitudes than SCD male mice (c-e). IJPs were elicited by single stimulus (train duration, 500 ms; frequency, 10 Hz; pulse duration, 0.8 ms; and voltage, 100 V) delivered by two parallel stimulating steel electrodes in the recording chamber. They were measured using glass electrodes penetrating into the circular muscle of muscularis externa from the mucosal surface.

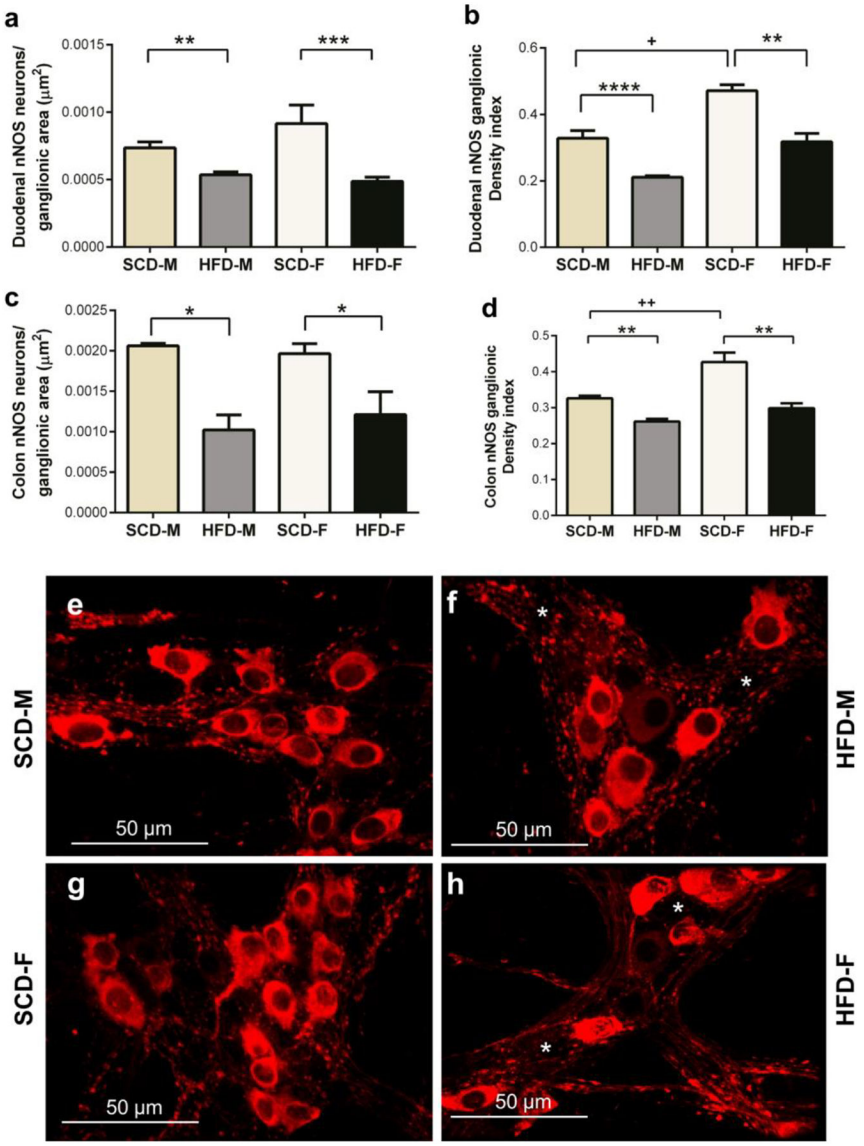

Fig. 3.

HFD reduces intestinal nitrergic myenteric neurons in both male and female mice. In both duodenum and colon, HFD mice of both sexes had lower numbers of nNOS neurons per ganglionic area than SCD mice (a, c). Likewise, the overall amount of nNOS immunoreactivity (area of stained neurons and varicosities per ganglion area; density index) was reduced in HFD mice of both sexes (b, d). nNOS immunoreactivity was higher in SCD female mice than SCD male mice (b, d). Pictures are sample images showing nNOS staining in colon myenteric ganglia of SCD-M (e), HFD-M (f), SCD-F (g) and HFD-F (h) mice. F and h show fewer nNOS neurons compared to e and g, respectively. White asterisks indicate areas of reduced nNOS immunoreactivity.

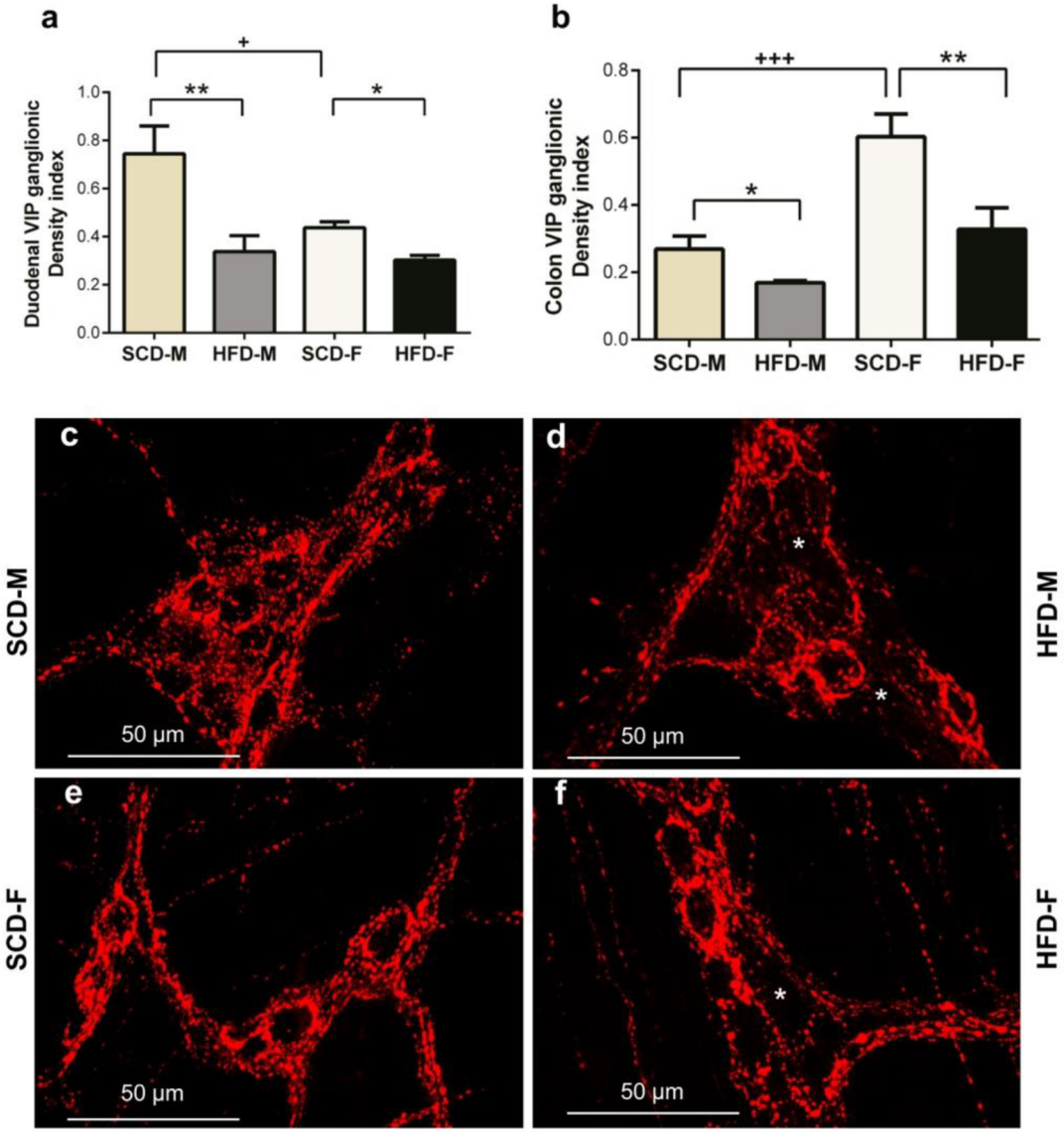

Fig. 4.

HFD reduces myenteric VIP immunoreactive varicosities in the myenteric plexus in both male and female mice intestines. Similar to nNOS data, SCD male and female mice had higher VIP immunoreactivity in the duodenum and colon than HFD male and female mice (a-b). SCD female mice had higher VIP immunoreactivity in the colon than SCD male mice (b), but male SCD mice had higher VIP immunoreactivity in the duodenum than female SCD mice (a). Pictures are sample images showing VIP staining in SCD-M (c), HFD-M (d), SCD-F (e) and HFD-F (f) mice duodenal myenteric plexus. White asterisks show areas of reduced VIP varicosities (d, f).

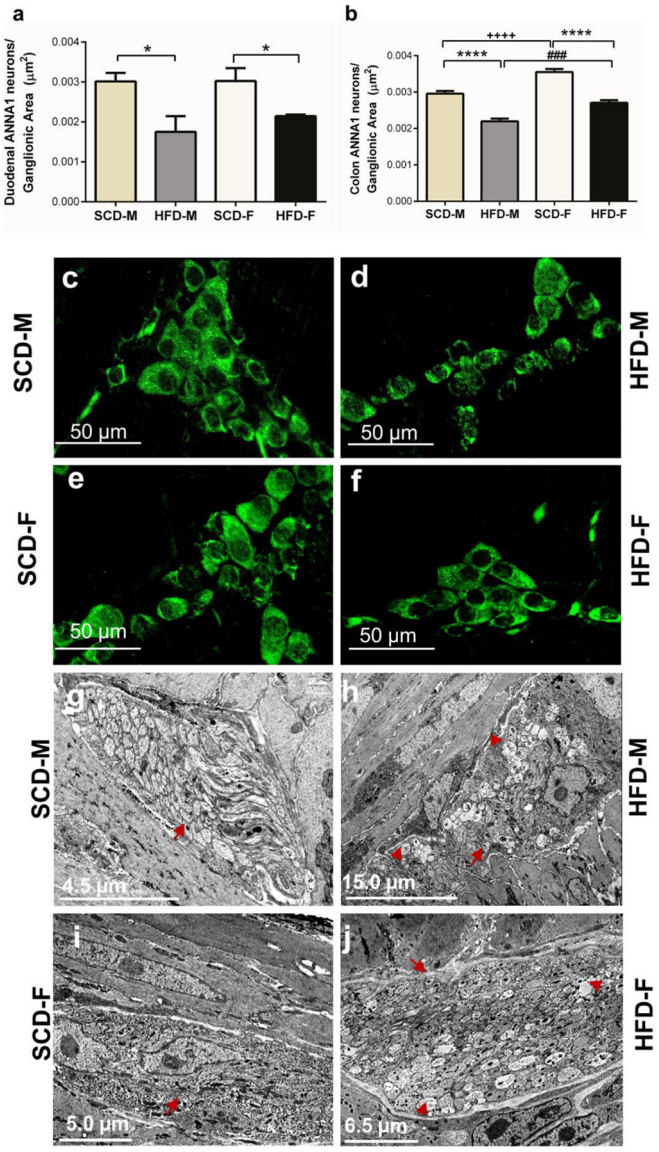

Fig. 5.

HFD reduces the total number of myenteric neurons, and causes axonal swelling and loss of cytoskeletal filaments in the myenteric plexus in both male and female mice. The total number of neurons labeled with ANNA-1 per ganglionic area was reduced in both male and female mice fed HFD in the duodenum (a) and colon (b). Images of neurons stained by ANNA-1 immunohistochemistry in SCD-M (c), HFD-M (d), SCD-F (e) and HFD-F (f) mice duodenal myenteric plexus. TEM images of SCD (g, i) and HFD (h, j) male and female mice duodenum demonstrate ultrastructural HFD-induced nerve injury. This includes axonal swelling and loss of neurofilaments and microtubules. Red arrows show healthy axons and swollen axons with disrupted neurofilaments and arrowheads indicate microtubules.

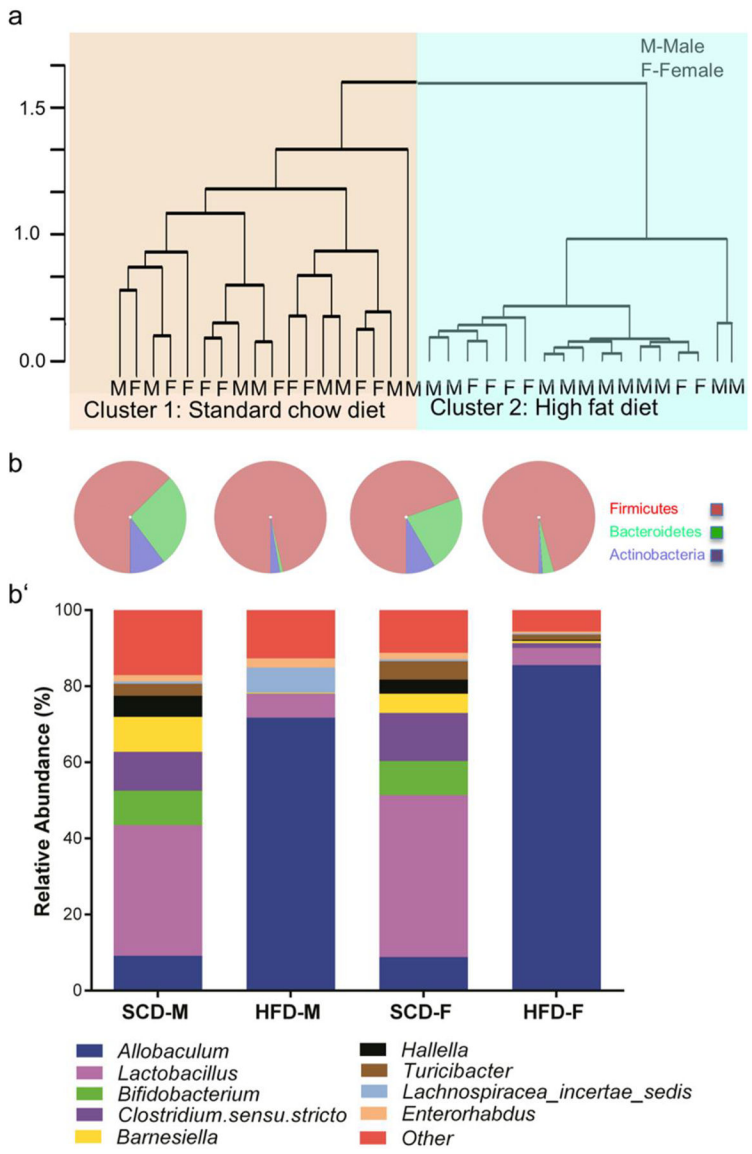

Fig. 6.

HFD is the primary determinant of gut bacterial community composition. Hierarchical clustering revealed samples grouped together by diet and not by sex (a). The abundance of identified bacteria belonging to the phylum Firmicutes was dramatically increased in HFD mice, while Bacteroidetes and Actinobacteria were reduced by HFD ingestion (b). Stacked bar graphs show specific gut bacteria affected by HFD ingestion regardless of sex (c). Among increased genera, *Allobaculum* was the most prominent, while *Lactobacillus*, *Clostridium sensu stricto*, and *Bifidobacterium* were prominently decreased by HFD ingestion. *For clarity, bacteria with less than 1% relative abundances were grouped and labeled "*Other*". Further details on bacteria labeled *"Other"* may be found on Supplementary Table S7.

Table 1:

Bacterial genera * that show significant correlations with intestinal motility, neuropathy or both in duodenum and colon.

	Duodenal velocity		Duodenum nNOS[a]		Colon Velocity		Colon nNOS[a]	
Organism	**P value**	**Pearson's r**	**P value**	**Pearson's r**	**P value**	**Pearson's r**	**P value**	**Pearson's r**
Allobaculum[#]	0.002	−0.998	0.043	−0.957	0.063	−0.937	0.044	−0.956
Lactococcus[#]					0.078	−0.922	0.020	−0.980
Bifidobacterium[+]	0.012	0.988	0.047	0.953	0.043	0.957	0.013	0.987
Butyrivibrio[+]	0.010	0.990	0.051	0.949	0.040	0.960	0.013	0.987
Hallella[+]	0.038	0.962	0.163	0.837	0.000	1.000	0.026	0.974
Anaerobacter[+]	0.055	0.945	0.024	0.976				
Clostridium.sensu.stricto[+]	0.048	0.952	0.022	0.978				
Lactobacillus[+]	0.033	0.967	0.008	0.992				
TM7_genera_in certae_sedis[+]	0.050	0.950	0.059	0.941				

[a] nNOS here refers to the number of nNOS neurons per ganglionic area.

[*] Only bacterial genera with relative abundances greater than 1% are shown on this table. A detailed list of all organisms with significant correlations to enteric neuropathy and motility may be found in supplementary Tables S2–5.

[#] These are bacteria increased by HFD ingestion in both male and female mice.

[+] These are bacteria decreased by HFD ingestion in both male and female mice.